

# Computational Study of the Effects of AF-related Genetic Mutations in 3D Human Atrial Model

Rebecca Belletti<sup>1</sup>, Lucia Romero<sup>1</sup>, Javier Saiz<sup>1</sup>

<sup>1</sup>Centro de Investigación e Innovación en Bioingeniería, Universitat Politècnica de València, Valencia, Spain

## Abstract

Atrial fibrillation (AF) is the most frequent atrial rhythm disorder with an incidence increasing with age. Genetic mutations impairing the normal functioning of  $I_{Kr}$  and  $I_{to}$  channels are implicated in AF outbreaks in healthy patients. The higher susceptibility to AF in presence of *KCNH2 T436M*, *KNCH2 T895M* and *KCNE3-V17M* mutations was previously studied by simulating their effects on atrial electrophysiology in single-cell and tissue. This work aims at extending the previous study to a 3D bi-atrial model to assess vulnerability to AF initiation and maintenance on a complex geometry. A realistic model of human atria was used to run 3D simulations and study temporal vulnerability. After stabilization, a train of stimuli was applied to the coronary sinus region to simulate an ectopic stimulus and to induce arrhythmia. The results show a higher susceptibility of the mutant atria to develop arrhythmias in a mutation-dependent fashion. The *KCNE3-V17M* variant was the most pro-arrhythmogenic with a 24ms-wide vulnerable window (VW) and instable arrhythmic patterns. The *KNCH2 T895M* and *KCNH2 T436M* mutations presented a VW of 7ms and 10ms, respectively, with mainly macro re-entries. These findings highlight the different effects of the genetic mutations and the importance of a patient-specific approach.

## 1. Introduction

Atrial fibrillation (AF) is the most common supraventricular tachyarrhythmia affecting the upper chambers of the heart. AF is responsible for chaotic and asynchronous atrial electrical activations, resulting in inefficient heart contraction and a 3.5-fold higher risk of thromboembolic stroke by blood clots formations. AF prevalence in adults is around 2-4% and increases with age. Among many others comorbidities and risk factors associated to AF, genetic predisposition plays an important role in AF onsets, progression and maintenance

in asymptomatic and apparently healthy patients [1]. Genetic mutations affecting the genes encoding potassium channel protein structure directly affect the repolarization phase of cardiac cells electrophysiology. These changes result in a shortening or lengthening of the effective refractory period (ERP), hence increasing the vulnerability to AF [2], [3]. The use of computational modelling can considerably help to improve the understanding of physiological and pathological atrial properties [4]. The effects of three gain-of-function mutations – *KNCH2 T436M*, *KCNH2 T895M* and *KCNE3-V17M* – have been investigated at single-cell and tissue level using computational models [5]. These three genetic mutations, affecting the normal functioning of rapid delayed and transient outward  $K^+$  channels, proved to increased cellular and tissue vulnerability to AF initiation and sustainability. The aim of this work is to study the vulnerability to AF of such mutations on a three dimensional scale by using 3D models of human atrial geometry.

## 2. Material and Methods

### 2.1. 3D geometrical model

The human atrial model used in this study is a three-dimensional hexahedral mesh composed by 751691 nodes and 512828 elements. It is characterized by 56 regions that allows to account for the differences in histological properties and in fibre orientation, and presents a spatial resolution of 300  $\mu\text{m}$  [6], [7].

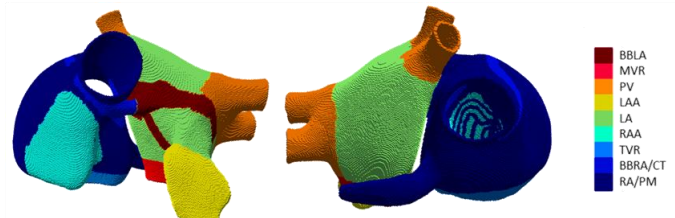


Figure 1. 3D atrial model with the nine corresponding color-coded ionic models.

The cellular electrical activity was simulated using a modified version of the Courtemanche-Ramirez-Nattel (CRN) human atrial model, which includes the acetylcholine-activated  $K^+$  current (with  $[ACh] = 0.005 \mu M$ ) from the Grandi model to take into account the effects of the autonomic nervous system [8]–[10]. Moreover, the CRN model was modified to reproduce the effects of the three genetic mutations, thus resulting into 3 different versions of the CRN model, one for each mutant case. The  $I_{Kr}$  and  $I_{to}$  current formulations were modified as shown in equations (1) to (6)

$$\alpha_{xr} = 0.0003 \frac{V+14.1}{1-e^{-5}} \quad (1)$$

$$\beta_{xr} = p_{1r} \cdot 7.3898 \cdot 10^{-5} \frac{V-3.3328+p_{2r}}{e^{\frac{V-3.3328+p_{2r}}{5.1237 \cdot p_{3r}}}-1} \quad (2)$$

$$I_{Kr} = C_m \cdot p_{4r} \cdot g_{Kr} \cdot \alpha_r \frac{V-Ek}{1+e^{22.4 \cdot p_{5r}}} \quad (3)$$

$$\alpha_{oi} = \frac{p_{1t}}{18.53+e^{10.95 \cdot p_{2t}}} \quad (4)$$

$$\beta_{oi} = \frac{p_{3t}}{35.56+e^{-7.44 \cdot p_{4t}}} \quad (5)$$

$$I_{to} = C_m \cdot p_{5t} \cdot g_{to} \cdot \alpha_i \cdot \alpha_a^3 (V - Ek) \quad (6)$$

and parameters' values were defined as follows: the parameters  $p_{1r}$ ,  $p_{2r}$ ,  $p_{3r}$  and  $p_{4r}$  were set respectively to 1.08, 46.96, 4.64 and 1.41 to reproduce the changes provoked by the mutation KCNH2 T436M and to 2.134, 51.14, 3.49 and 1.99 to replicate the effects of the mutation KCNH2 T895M on the  $I_{Kr}$ . Finally, the alterations caused by the KCNE3-V17M mutation were reproduced employing two separate sets of parameters, each one acting on a different ionic current formulation. The parameters  $p_{1r}$ ,  $p_{4r}$  and  $p_{5r}$  were used to modify the  $I_{Kr}$  formulation with values 0.51, 6.18 and 0.71. At the same time, the parameters  $p_{1t}$ ,  $p_{2t}$ ,  $p_{3t}$ ,  $p_{4t}$  and  $p_{5t}$  were included in the  $I_{to}$  formulation and were set to 2, 1.87, 8.14, 0.68 and 12.56, respectively. Regional heterogeneity of the electrical properties in the atria were taken into account by tuning some ionic channel conductances, thus generating nine different electrical version of every mutated model (Table 1). The values of longitudinal conductivity and anisotropy ratio were also tuned to replicate the heterogeneity in atrial tissues' conductivities and to reproduce the physiological sequence of activation.

Table 1. Ionic channel conductances changes associated to the nine different regional models. RA: right atrium. CT-BBra: crista terminalis – right atrium Bachmann bundle. BBla: left atrium Bachmann bundle. TVR: tricuspid valve ring. MVR: mitral valve ring. RAA: right atrium appendage. LAA: left atrium appendage. LA: left

atrium. PV: pulmonary vein.

	$g_{K1}$	$g_{to}$	$g_{Kr}$	$g_{Ks}$	$g_{CaL}$
<b>RA</b>	1	1	1	1	1
<b>CT-BBra</b>	1	1	1	1	1.67
<b>BBla</b>	1	1	1.6	1	1.67
<b>TVR</b>	1	1	1.3	1	0.8
<b>MVR</b>	1	1	2.6	1	0.8
<b>RAA</b>	1	0.68	1.1	1	0.9
<b>LAA</b>	1	1	2.2	1	0.9
<b>LA</b>	1	1	2	1	0.9
<b>PV</b>	0.9	0.9	2.5	1.9	0.8

The 3D atria model was first stabilized by applying a train of 10 stimuli at the sinoatrial node (SAN) at a basic cycle length of 1000 ms to smoothen the electrical differences among the nine electrophysiological regions [11]. Then, a train of 5 pulses was then applied at the coronary sinus (CS) region to simulate ectopic activation of the atria and induce the arrhythmic behaviour. The BCLs of the ectopic beats depended one each mutation accordingly with their effects on the ERP. Thus, the BCL was 160 ms for the KCNH2 T436M mutation, 170 ms for the KCNH2 T895M mutation and, finally, 90 ms for the KCNE3-V17M mutation. In the Wild-Type (WT) case, all the three BCLs were applied for the sake of comparison. During the ectopic stimulation, the activity of the SAN was maintained with a BCL of 1000 ms. Thus, after the 10 stimuli given at the SAN, other five seconds of electrical activity were simulated. The temporal vulnerability of the atria to fibrillatory activity was quantified by computing the vulnerable window (VW) width for each mutation, as the time window (in ms) in which a 5 pulses train applied at the CS region would initiate an arrhythmia completing at least two cycles around the atria. The monodomain formalism was solved using the Elvira software with a time step of 0.01 ms [12].

### 3. Results

Susceptibility to arrhythmia of the three genetic mutations under study – KCNH2 T436M, KCNH2 T895M and KCNE3-V17M – was characterized by assessing temporal vulnerability to AF. Differences in vulnerability to arrhythmia initiation and maintenance, in vulnerable windows' widths and in the type of fibrillatory patterns elicited could be observed comparing the three cases studied. In presence of the KCNE3-V17M mutation, the atria turned out to be much more vulnerable to AF initiation, followed by the KCNH2 T895M and KCNH2 T436M mutations, as show in Figures 2-4. In presence of the KCNH2-T436M mutation, the computed VW was 10ms-wide, as shown in Figure 2; during this time frame, 90% of induced arrhythmias were macro re-

entries, whilst the remaining 10% were characterized by rotor anchoring in the right atrium (RA) wall (Figure 4) (Figure 3). In general, fibrillatory patterns perpetuated from a minimum of 3.8 s to a maximum of 5 s.

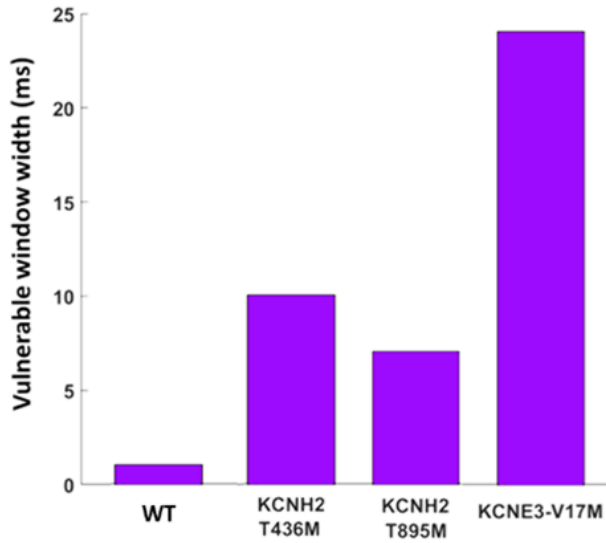


Figure 2. Width of the vulnerable windows for each case.

For the KCNH2 T895M mutation, a VW of 7 ms was observed (Figure 2). In this case, only macro re-entries were elicited and they perpetuated from a minimum of

induced in the 79% of the VW. The arrhythmic episodes were characterized by the formations and collisions of many rotors with wave breaks and an overall instable dynamic. The remaining 21% of the width of the VW was characterized by the generation of a single rotor arising in the CS region and moving around the RA wall (Figure 2 and 3). Finally, in the WT scenario, a 1ms-wide VW was observed, just when pacing the CS region with a BCL = 170 ms (Figure 2). As shown in Figure 3, susceptibility to arrhythmia initiation depends on the mutation case under study.

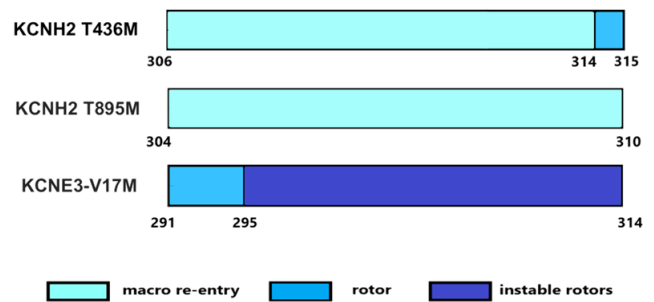


Figure 3. Temporal vulnerability of the atria to arrhythmia generation in the presence of the KCNH2 T436M, KCNH2 T895M, and KCNE3-V17M mutations. Different arrhythmic patterns are color-coded as shown in the legend.

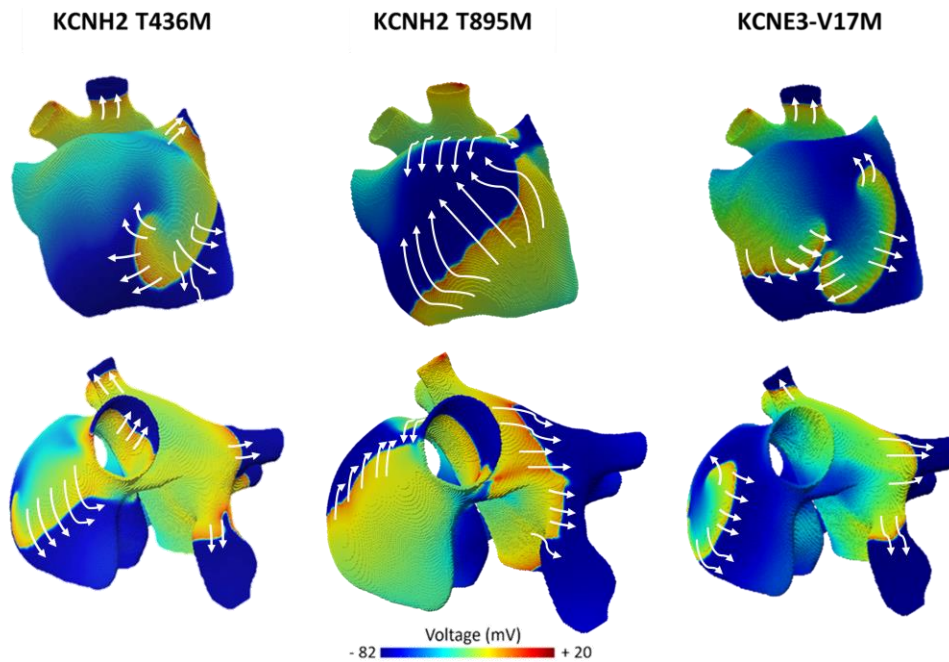


Figure 4. 3D simulation of different arrhythmic behaviors in the presence of KCNH2 T436M, KCNH2 T895M and KCNE3-V17M mutations. The white arrows indicate the direction of propagation.

In this work, the effects of three gain-of-function mutations previously studied at cellular and tissue levels have been investigated using a 3D human bi-atrial model. The three mutations – KCNH2 T436M, KCNH2 T895M and KCNE3-V17M – affecting the gene encoding  $I_{Kr}$ 's and  $I_{to}$ 's channel protein structures, were integrated into the CRN human atrial model by reparametrizing the corresponding current formulations. Then, 3D computer simulations of the human atrial model were run including the mutant variants and heterogeneous regional electrical properties and conductivities. After electrically stabilizing the atrial model by applying a train of 10 pulses to the SAN, the onset of arrhythmic behaviour was induced by pacing the CS region with a train of 5 pulses. Susceptibility to AF initiation and maintenance was thus studied by computing the temporal vulnerability. The three genetic mutations led to a much more arrhythmogenic substrate than WT, favouring the onset of arrhythmic behaviour and sustained fibrillations. Accordingly with previous results, the KCNE3-V17M mutation turned out to be the most pro-arrhythmogenic mutation among the three studied at 3D level; in fact, it had the widest VW and produced the highest number of complex arrhythmogenic patterns characterized by instable rotors, multiple collisions and wave breaks. Moreover, the coupling intervals inducing AF were the shortest due to the shortest ERP. On the other hand, the KCNH2 T436M and KCNH2 T895M mutations presented a comparable behaviour respect to each other, with a smaller vulnerable window and by inducing mainly macro re-entries. These two latter mutations led to the formation of a much less vulnerable substrate when compared with the KCNE3-V17M mutation. Thus, the differences among induced arrhythmic patterns highlighted even more the underlying distinct substrate generated by the mutations.

## Acknowledgments

I acknowledge this work to the European Union's Horizon 2020 research and innovation programme under the Marie Skłodowska-Curie grant agreement No.766082 and to the Dirección General de Política Científica de la Generalitat Valenciana (PROMETEO/2020/043).

## References

[1] G. Hindricks *et al.*, “2020 ESC Guidelines for the diagnosis and management of atrial fibrillation developed in collaboration with the European Association for Cardio-Thoracic Surgery (EACTS),” *Eur. Heart J.*, vol. 42, no. 5, pp. 373–498, 2021, doi: 10.1093/eurheartj/ehaa612.

[2] A. A. Y. Ragab, G. D. S. Sitorus, B. B. J. J. M. Brundel, and N. M. S. de Groot, “The Genetic Puzzle of Familial Atrial Fibrillation,” *Front. Cardiovasc.*

*Med.*, vol. 7, no. February, pp. 1–8, 2020, doi: 10.3389/fcvm.2020.00014.

[3] J. Feghaly, P. Zakka, B. London, C. A. Macrae, and M. M. Refaat, “Genetics of Atrial Fibrillation,” *J. Am. Heart Assoc.*, vol. 7, pp. 1–15, 2018, doi: 10.1161/JAHA.118.009884.

[4] O. Dössel, M. W. Krueger, F. M. Weber, M. Wilhelms, and G. Seemann, “Computational modeling of the human atrial anatomy and electrophysiology,” *Med. Biol. Eng. Comput.*, vol. 50, no. 8, pp. 773–799, 2012, doi: 10.1007/s11517-012-0924-6.

[5] R. Belletti, L. Romero, L. Martinez-Mateu, E. M. Cherry, F. H. Fenton, and J. Saiz, “Arrhythmogenic Effects of Genetic Mutations Affecting Potassium Channels in Human Atrial Fibrillation: A Simulation Study,” *Front. Physiol.*, vol. 12, no. May, pp. 1–16, 2021, doi: 10.3389/fphys.2021.681943.

[6] S. Rocher, L. Martinez, A. Lopez, A. Ferrer, D. Sanchez-Quintana, and J. Saiz, “A Three-Dimensional Model of the Human Atria With Heterogeneous Thickness and Fibre Transmurality - A Realistic Platform for the Study of Atrial Fibrillation,” *2019 Comput. Cardiol. Conf.*, vol. 45, pp. 2019–2022, 2019, doi: 10.22489/cinc.2019.380.

[7] A. Ferrer *et al.*, “Detailed anatomical and electrophysiological models of human atria and torso for the simulation of atrial activation,” *PLoS One*, vol. 10, no. 11, pp. 1–29, 2015, doi: 10.1371/journal.pone.0141573.

[8] M. Courtemanche, R. J. Ramirez, and S. Nattel, “Ionic mechanisms underlying human atrial action potential properties: insights from a mathematical model,” *Am. J. Physiol. -Heart Circ. Physiol.*, vol. 275, pp. 301–321, 1998, doi: 10.1152/ajpheart.1998.275.1.H301.

[9] E. Grandi *et al.*, “Human atrial action potential and Ca<sup>2+</sup> model: Sinus rhythm and chronic atrial fibrillation,” *Circ. Res.*, vol. 109, no. 9, pp. 1055–1066, 2011, doi: 10.1161/CIRCRESAHA.111.253955.

[10] D. Dobrev and U. Ravens, “Remodeling of cardiomyocyte ion channels in human atrial fibrillation,” *Basic Res. Cardiol.*, vol. 98, no. 3, pp. 137–148, 2003, doi: 10.1007/s00395-003-0409-8.

[11] L. Martinez-Mateu *et al.*, “Factors affecting basket catheter detection of real and phantom rotors in the atria: A computational study,” *PLoS Comput. Biol.*, vol. 14, no. 3, pp. 1–26, 2018, doi: 10.1371/journal.pcbi.1006017.

[12] E. A. Heidenreich, J. M. Ferrero, M. Doblaré, and J. F. Rodríguez, “Adaptive macro finite elements for the numerical solution of monodomain equations in cardiac electrophysiology,” *Ann. Biomed. Eng.*, vol. 38, no. 7, pp. 2331–2345, 2010, doi: 10.1007/s10439-010-9997-2.

Address for correspondence:

Rebecca Belletti.  
 Universitat Politècnica de Valencia, Camí de Vera s/n, 46022,  
 Valencia, Valencia, España  
[rbelletti@ci2b.upv.es](mailto:rbelletti@ci2b.upv.es)